RSC Advances

PAPER

View Article Online
View Journal | View Issue



Cite this: *RSC Adv.*, 2021, **11**, 21986

# Electrocatalytic carboxylation of halogenated compounds with mesoporous silver electrode materials†

Si-Li Shan, Cheng-Jie Jiang, Yu-Ting Liu, Jing-Jie Zhang, Huan Wang* and Jia-Xing Lu *

Received 1st April 2021
Accepted 6th June 2021

DOI: 10.1039/d1ra02563e

rsc.li/rsc-advances

Mesoporous silver materials are used as electrocatalysts for halogenated compounds. The mesoporous silver materials have uniform mesoporous size (8 nm), large specific surface area (12 $m^2\ g^{-1}$), high pore volume (0.07 $cm^3\ g^{-1}$), and a good 3D network structure of the metallic silver skeleton. The results show that the prepared materials exhibit high performance in electrocatalytic carboxylation of halogenated compounds to acid (78%).



The main factor of global warming and the greenhouse effect is the increase of concentration of carbon dioxide ($CO_2$).[1,2] There are two ways to solve the problem of $CO_2$ concentration. The first method is to establish a low-carbon economic development model. The second method is to convert $CO_2$ into useful organic chemicals.[3,4] As human production and life are inseparable from the use of fossil fuels, the problem of $CO_2$ emissions will still exist. Therefore, today's society urgently pays attention to how to effectively transform and utilize $CO_2$; in addition, the conversion of $CO_2$ into productive products has attracted widespread attention.[5,6] $CO_2$ conversion is a challenge because of its high chemical and thermodynamic stability. Through electrochemical means, $CO_2$ can be activated at normal temperature and pressure.[7] Therefore, from the perspective of environmental protection and technical means, electrocarboxylation is a simple and easy method for $CO_2$ immobilization. Electrocatalytic carboxylation can be applied to a variety of substrates, such as olefins,[8] alkynes,[9] alcohols,[10] aldehydes,[11] ketones,[12] epoxides,[13] imines[14] and organic halides.[15] Halogenated compounds are toxic, carcinogenic and difficult to biodegrade. Electrocarboxylation of halogenated compounds not only immobilizes $CO_2$ and reduces environmental pollution, but also converts them into useful compounds. More importantly, several of them are fine chemicals with industrial use, and some of them can produce anti-influenza drugs, such as benzoic acid, sodium benzoate, benzyl benzoate *etc.*[16]

Silver shows remarkable electrocatalytic activity when it is used for electrocarboxylation of organic halides.[17] In addition, silver nanoparticles have been used in electrocatalytic reactions. In the field of electrocatalysis using silver nanoparticles, researchers have made great efforts. Firstly, a silver nanoparticle-modified electrode was successfully prepared and applied to electrocatalytic reduction of benzyl chloride.[18] At the same time, through the electrochemical detection method, the catalytic activity of the nano silver modified electrode was compared with the silver electrode, and the catalytic activity of the modified electrode after repeated use was discussed. Simonet *et al.* electrodeposited silver nanoparticles on glassy carbon electrode, and explored a variety of organic halogenated compounds to study the universality of nano silver-modified electrodes in electrocatalytic reduction of organic halides.[19]

On the other hand, numerous research efforts have been reported to control the morphology of metal nanoporous materials to obtain optimized activity in electrocatalysis. Mesoporous silver material has the advantages of large specific surface area, large pore volume, regular mesoporous structure, good chemical inertia, good ductility, good thermal stability and good conductivity, so it has been widely concerned. These properties are beneficial to heterogeneous catalytic reactions and other applications, such as adsorption/separation, fuel cells and biosensors.[20] However, mesoporous silver materials are mainly used to enhance the reproducibility and sensitivity of Raman scattering signals,[21] and are rarely used in electrocarboxylation. How to improve the yield of electrocarboxylation by using mesoporous silver electrode and expand the application range of mesoporous silver materials is worthy of our efforts.

In this study, we used hard template method to synthesize mesoporous silver for electrocatalytic carboxylation of halogenated compounds. Different mesoporous silver materials are obtained by adjusting the amount of silver nitrate solution.

The experimental results show that mesoporous silver with different mesoporous pore sizes has different catalytic

*Shanghai Key Laboratory of Green Chemistry and Chemical Processes, School of Chemistry and Molecular Engineering, East China Normal University, Shanghai, 200062, China. E-mail: hwang@chem.ecnu.edu.cn; jxlu@chem.ecnu.edu.cn*

† Electronic supplementary information (ESI) available. See DOI: 10.1039/d1ra02563e

performance on the electrocatalytic carboxylation of halogenated compounds to acid under mild conditions.

A series of mesoporous silver was synthesized by using hydrophobic mesoporous silica KIT-6 as template and silver nitrate as metal precursor (see the ESI† for details),[22] which are named as mesoAg-1, mesoAg-2, mesoAg-3, mesoAg-4 and mesoAg-5. The X-ray diffraction (XRD) patterns (Fig. 1) show that these five materials all have four characteristic peaks at 38.0°, 44.3°, 64.5° and 77.3° respectively, corresponding to the (111), (200), (220) and (311) face centered cubic crystal faces of the standard card PDF # 04-0783 of Ag, which indicates that these materials are metallic silver.

Morphologies of mesoporous silver materials were characterized by scanning electron microscope (SEM) and transmission electron microscope (TEM). As shown in Fig. 2, mesoAg-3 material is composed of many nanoparticles with a diameter of 8 nm, which is close to the pore size of HP-KIT-6 template (Table S1 and Fig. S1†). This indicates that the mesoporous structure of the template has been well duplicated. The morphologies of mesoporous silver prepared with the same quality template and different quality of silver nitrate solution are different (Fig. 2b and S2†). The regular arrangement of mesoporous silver can be observed in the SEM images of mesoAg-3 and mesoAg-4. Moreover, the accumulation of silver in mesoAg-3 and mesoAg-4 is less than that of other three materials. In the SEM images of mesoAg-1, mesoAg-2 and mesoAg-5, not only the mesoporous structure of silver but also the accumulation of silver could be observed. It's probably because in the process of preparing mesoporous silver, adding too much or too little silver nitrate solution will lead to incomplete replication of the mesoporous structure, resulting in larger particle size. If the mass of $AgNO_3$ solution is too much, it will lead to solution outside the template channel. Due to surface tension, part of the solution that should have been immersed in the channel will also be attracted to the outside of the channel. In addition, during the thermal decomposition process of preparing mesoporous silver, that is, the sample was heated to 573 K under nitrogen flow for 2 hours, the mesoporous structure of silver is only formed in the mesoporous of the template. However, the silver outside the template is easy to grow into large particles, resulting in the formation of massive silver.[22] While the mass of $AgNO_3$ solution is too small, although

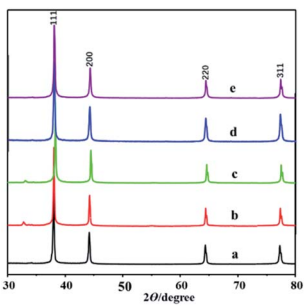


Fig. 1 XRD patterns of (a) mesoAg-5, (b) mesoAg-4, (c) mesoAg-3, (d) mesoAg-2 and (e) mesoAg-1.

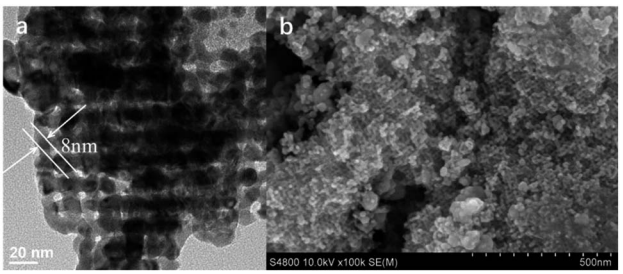


Fig. 2 (a) TEM and (b) SEM images for mesoAg-3.

the solution will exist in the channel, the channel is not completely saturated and the mesoporous structure is not completely replicated. These two conditions lead to the decrease of silver content in the mesoporous template, the formation of silver mesoporous structure is less, which may lead to the decrease of specific surface area and pore volume.

$N_2$ adsorption desorption isotherms and corresponding BJH pore size distribution curves were measured for mesoporous silver materials (Fig. 3 and S3†). As shown in Fig. 3, both mesoAg-3 and mesoAg-4 have obvious IV adsorption isotherms and H1 hysteresis loops in the specific pressure range of 0.45–0.75, which indicates that both samples have mesoscopic pore structure. H3 hysteresis loops appeared for mesoAg-1, mesoAg-2 and mesoAg-5, indicating that there are mutual accumulations of mesoporous silver in the materials, and the pore structure became irregular. It is consistent with SEM image (Fig. S2†). Textural parameters of these mesoporous silver materials are summarized in Table 1. It can be found that the average pore sizes of mesoAg-1, mesoAg-2 and mesoAg-5 are above 50 nm, while those of mesoAg-3 and mesoAg-4 are within 10 nm. The mesoporous structures of mesoAg-1, mesoAg-2 and mesoAg-5 are less than those of mesoAg-3 and mesoAg-4 and the mesoporous structures of the three materials are stacked more. The specific surface area and pore volume of the last two mesoporous materials are larger than those of the first three

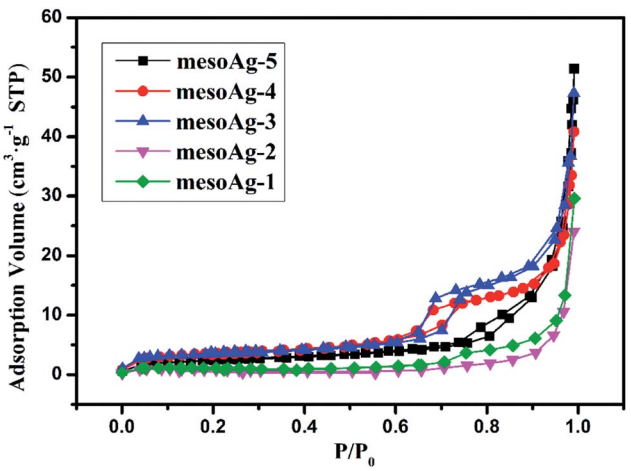


Fig. 3 $N_2$ adsorption–desorption isotherms for the mesoporous silver materials.

Table 1 Structure parameters for mesoporous Ag

| Entry | Material | BET surface area[a] ($m^2\ g^{-1}$) | Total pore volume[b] ($cm^3\ g^{-1}$) | Average pore size[c] (nm) |
|---|---|---|---|---|
| 1 | mesoAg-1 | 4 | 0.04 | 79.5 |
| 2 | mesoAg-2 | 3 | 0.04 | 68.9 |
| 3 | mesoAg-3 | 12 | 0.07 | 8.0 |
| 4 | mesoAg-4 | 12 | 0.06 | 7.1 |
| 5 | mesoAg-5 | 9 | 0.07 | 145.1 |

[a] BET surface areas calculated from the $N_2$ adsorption branches in the range of relative pressure ($p/p_0$) = 0.05–0.20. [b] Total pore volumes measured at $p/p_0$ = 0.99. [c] Pore diameters obtained from $N_2$ adsorption branches by BJH method.

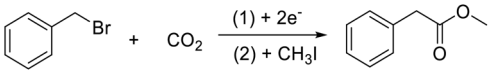


Scheme 1 Electrocarboxylation of benzyl bromide under $CO_2$ atmosphere.

materials, and the specific surface area and pore volume of mesoAg-3 are the largest. With the decrease of the mass of silver nitrate solution added in the preparation process, the specific surface area of the material first increases and then decreases. The surface of the material is an important place for the reaction, the mesoporous structure has a large specific surface area and pore volume, which can provide a large space for the reaction to be fully carried out, so the catalytic efficiency may be increased. Therefore, it can be inferred that mesoAg-3 has the highest catalytic efficiency.

The electrocarboxylation of halogenated compounds is to break the carbon halide bond in the halide by electrochemical method, so as to remove the halogen atom, and then react with $CO_2$ to form corresponding carboxylic acid compounds. Now we have been able to carboxylate a variety of organic halides, such as halogenated benzyl, by electrocatalytic method. In order to explore the effect of materials on electrocatalytic carboxylation of halogenated compounds, benzyl bromide was used as a model compound (Scheme 1).

The yields of electrocarboxylation of benzyl bromide using different mesoporous silver are shown in Table 2. The yield of methyl phenylacetate was 17% on a flat silver electrode (Table 2, entry 1). 78% and 69% yields can be obtained on mesoAg-3 and mesoAg-4, respectively, which is 4.6–4.1 times higher than that on flat silver electrode (Table 2, entries 4 and 5). Using mesoAg-1, mesoAg-2 and mesoAg-5, the yields were 25%, 33% and 34%, respectively (Table 2, entries 2, 3 and 6). The above data show that electrocatalytic properties of the five mesoporous silver materials are better than that of the flat silver, and the yields on mesoAg-3 and mesoAg-4 are higher than those on mesoAg-1, mesoAg-2 and mesoAg-5. MesoAg-3 is the best among the five mesoporous silvers. It is known that the specific surface area and pore volume of mesoAg-3 and mesoAg-4 materials are larger than those of other three materials. These two materials can provide larger space for the full reaction in the catalytic process, so their catalytic efficiency is higher than those of other three materials.

For comparison, the other two silver materials, silver nanoparticles and foam silver, were tested (Table 2, entries 7–8). The yields on the two materials were 36% and 30%, respectively. From Table S2,† the specific surface area of silver nanoparticles

Table 2 The yield of methyl phenylacetate at different mesoporous silver materials[a]

| Entry | Substrate | Cathode | $Q$ ($F\ mol^{-1}$) | Yield[b] (%) |
|---|---|---|---|---|
| 1 | Benzyl bromide | Silver plate | 2 | 17 |
| 2 | Benzyl bromide | mesoAg-1 | 2 | 25 |
| 3 | Benzyl bromide | mesoAg-2 | 2 | 33 |
| 4 | Benzyl bromide | mesoAg-3 | 2 | 78 |
| 5 | Benzyl bromide | mesoAg-4 | 2 | 69 |
| 6 | Benzyl bromide | mesoAg-5 | 2 | 34 |
| 7 | Benzyl bromide | Silver nanoparticles | 2 | 36 |
| 8 | Benzyl bromide | Foam silver | 2 | 30 |
| 9 | Benzyl bromide | mesoAg-3 | 1.5 | 44 |
| 10 | Benzyl bromide | mesoAg-3 | 1.75 | 59 |
| 11 | Benzyl bromide | mesoAg-3 | 2.25 | 78 |
| 12 | Benzyl bromide | mesoAg-3 | 2.5 | 76 |
| 13 | 2-Phenylbromomethyl benzene | mesoAg-3 | 2 | 25 |
| 14 | 3-Phenylbenzyl bromide | mesoAg-3 | 2 | 36 |
| 15 | 4-Bromomethylbiphenyl | mesoAg-3 | 2 | 46 |

[a] General conditions: c(substrate) = 0.1 mol $L^{-1}$, DMF = 15 mL, c(TEABr) = 0.1 mol $L^{-1}$, $j$ = 2 mA $cm^{-2}$, $T$ = 25 °C, $P_{CO_2}$ = 1 atm, Mg as anode, electric charge = 2.0 F $mol^{-1}$. [b] GC yield.

and foam silver is 1.94 and 0.04 $m^2 g^{-1}$, respectively. As described above, the yield on the mesoAg-3 material is 78% and the specific surface area of mesoAg-3 material is 12 $m^2 g^{-1}$. The specific surface area of mesoAg-3 is the largest, and the specific surface area of foam silver is the smallest. Correspondingly, the catalytic efficiency of mesoAg-3 is the highest, and the catalytic efficiency of foamed silver is the lowest. This shows that a material with a small specific surface area cannot provide enough space for the reaction and has low catalytic efficiency.

Then the influence of electric charge amount was studied (Table 2, entries 4, 9–12). When the charge was in the range of 1.5–2 F $mol^{-1}$, the yield of methyl phenylacetate was increased with the increase in charge. When the charge exceeded 2 F $mol^{-1}$, the yield of methyl phenylacetate remained 78%. Moreover, the electrocarboxylation yields of other aromatic halides, 2-phenylbromomethyl benzene, 3-phenylbenzyl bromide and 4-bromomethylbiphenyl, were 25%, 36% and 46%, respectively (Table 2, entries 13–15). This indicates that mesoAg-3 electrode can effectively electrocatalytic carboxylation of aromatic halides.

After the reaction, the composite electrode was cleaned with solvent and used again in the next step under the same conditions. As shown in Fig. 4, even after 7 runs, the activity of the mesoporous silver materials does not decrease significantly, and the yield of methyl phenylacetate can be maintained at about 70%. In order to further study the stability of mesoAg-3 electrode, it was characterized by SEM after 7 times of use. As shown in Fig. 5, some silver particles in the used mesoAg-3 material are slightly larger than those before electrolysis. This may be due to the instability of the silver outside the template, it will agglomerate in the electrolysis process. The $N_2$ adsorption desorption isotherms and the corresponding BJH pore size distribution curves of mesoAg-3 electrode materials were shown in Fig. S4.† According to the $N_2$ adsorption desorption isotherms, there is obvious IV adsorption isotherm and H1 hysteresis loop in the specific pressure range of 0.45–0.75 before and after reuse, indicating that the material still has mesoporous structure after repeated use for 7 times. According to the BJH diagram, the peak appears at 8 nm before and after reuse, which indicates that the material is still a typical mesoporous material after 7 times of use. It can be seen from the data in Table S3† that the specific surface area of the material after reuse decreases. Due to the slight agglomeration, the specific surface area of the material after reuse decreases, resulting in a slight decrease in the electrolytic yield.

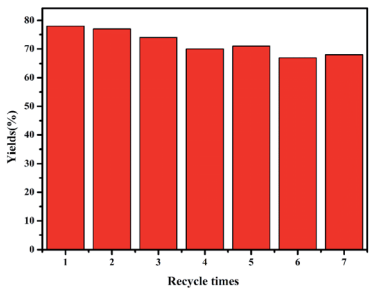


Fig. 4 Reuse of mesoporous silver cathode for electrocarboxylation of bromobenzyl.

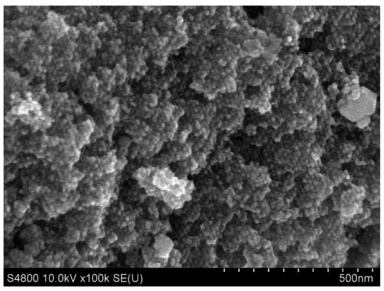


Fig. 5 SEM characterization of mesoporous silver cathode after bulk electrolysis.

## Conclusions

Electrocarboxylation of benzyl bromide can be achieved by using mesoporous silver for the first time under galvanostatic conditions. Through a series of experiments, it is found that the mesoporous silver prepared by adding appropriate amount of $AgNO_3$ solution has the most regular structure and the highest electrocatalytic performance. When the amount of $AgNO_3$ solution is too much or too little, the mesoporous structure of the prepared materials is stacked, and the electrocatalytic performance is lower than that of the former. The electrocatalytic effect of mesoporous silver was studied under different electrolytic charge and reactants. After 7 runs, the activity of the mesoporous silver materials does not decrease significantly, and the yield of methyl phenylacetate can be maintained at about 70% which indicates that mesoAg-3 electrode has the advantages of good stability.

## Conflicts of interest

There are no conflicts to declare.

## Acknowledgements

This work was financially supported by the National Natural Science Foundation of China (21773071, 22072046).

## Notes and references

1 C. M. Sánchez-Sánchez, V. Montiel, D. A. Tryk, *et al.*, *Pure Appl. Chem.*, 2001, **73**, 1917–1927.
2 M. Aresta and A. Dibenedetto, *Catal. Today*, 2004, **98**, 455–462.
3 T. Sakakura, J. C. Choi and H. Yasuda, *Chem. Rev.*, 2007, **107**, 2365–2387.
4 M. Mikkelsen, M. Jørgensen and F. C. Krebs, *Energy Environ. Sci.*, 2010, **3**, 43–81.
5 C. T. Dinh, T. Burdyny, M. G. Kibria, *et al.*, *Science*, 2018, **360**, 783–787.

6 S. Gao, Y. Lin, X. Jiao, Y. Sun, Q. Luo, W. Zhang, D. Li, J. Yang and Y. Xie, *Nature*, 2016, **529**, 68–71.
7 B. L. Chen, H. W. Zhu, Y. Xiao, Q. L. Sun, H. Wang and J. X. Lu, *Electrochem. Commun.*, 2014, **42**, 55–59.
8 S. N. Steinmann, C. Michel, R. Schwiedernoch, M. Wu and P. Sautet, *J. Catal.*, 2016, **343**, 240–247.
9 H. Wang, G. Zhang, Y. Liu, Y. Luo and J. Lu, *Electrochem. Commun.*, 2007, **9**, 2235–2239.
10 G. Q. Yuan, H. F. Jiang and C. Lin, *Tetrahedron*, 2008, **64**, 5866–5872.
11 M. Feroci, M. A. Casadei, M. Orsini, L. Palombi and A. Inesi, *J. Org. Chem.*, 2003, **68**, 1548–1551.
12 A. P. Doherty, *Electrochim. Acta*, 2002, **47**, 2963–2967.
13 A. Gennaro, A. A. Isse, J. M. Saveant, M. G. Severin and E. Vianello, *J. Am. Chem. Soc.*, 1996, **118**, 7190–7196.
14 K. H. M. Cardozo, R. Vessecchi, G. Ricardo, *et al.*, *J. Brazil. Chem. Soc.*, 2009, **20**, 1625–1631.
15 U. Hess and R. Thiele, *J. Prakt. Chem.*, 1982, **324**, 385–399.
16 P. P. Luo, Y. T. Zhang, *et al.*, *Catalysts*, 2017, **7**, 274.
17 A. A. Isse, L. Falciola, P. R. Mussini and A. Gennaro, *Chem. Commun.*, 2006, **3**, 344–346.
18 A. A. Isse, S. Gottardello, C. Maccato and A. Gennaro, *Electrochem. Commun.*, 2006, **8**, 1707–1712.
19 J. Simonet, *J. Appl. Electrochem.*, 2009, **39**, 1625–1632.
20 D. J. Guo and Y. Ding, *Electroanalysis*, 2012, **24**, 2035–2043.
21 C. F. Tian, J. Li and C. S. Ma, *Nanoscale*, 2015, **7**, 12318–12324.
22 J. K. Shon, S. S. Kong, J. M. Kim, C. H. Ko, *et al.*, *Chem. Commun.*, 2009, **45**, 650–652.